ARTICLE

ASCPT

Elevated acute phase proteins affect pharmacokinetics in COVID-19 trials: Lessons from the CounterCOVID - imatinib study

Imke H. Bartelink[1] | Pierre M. Bet[1] | Nicolas Widmer[2,3,4] | Monia Guidi[2,5] | Erik Duijvelaar[6] | Bram Grob[1] | Richard Honeywell[1] | Amanda Evelo[1] | Ivo P. E. Tielbeek[1] | Sue D. Snape[7] | Henrike Hamer[8] | Laurent A. Decosterd[2] | Harm Jan Bogaard[6] | Jurjan Aman[6] | Eleonora L. Swart[1]

[1]Department of Clinical Pharmacology and Pharmacy, Amsterdam UMC, location VUmc, Amsterdam, The Netherlands

[2]Service of Clinical Pharmacology, Lausanne University Hospital and University of Lausanne, Lausanne, Switzerland

[3]Specialised Centre for Emergency and Disaster Pharmacy, Institute of Pharmaceutical Sciences of Western Switzerland, University of Geneva, Geneva, Switzerland

[4]Pharmacy of the Eastern Vaud Hospitals, Rennaz, Switzerland

[5]Center for Research and Innovation in Clinical Pharmaceutical Sciences, Lausanne University Hospital and University of Lausanne, Lausanne, Switzerland

[6]Department of Pulmonary Medicine, Amsterdam Cardiovascular Sciences, Amsterdam UMC, location VUmc, Amsterdam, The Netherlands

[7]Exvastat Ltd., Cambridge, UK

[8]Department of Clinical Chemistry, Amsterdam UMC, location VUmc, Amsterdam, The Netherlands

Correspondence
Imke H. Bartelink, Department of Pharmacy, Amsterdam UMC, location VUmc, De Boelelaan 1117, 1081 HV Amsterdam, The Netherlands.
Email: i.bartelink@amsterdamumc.nl

Abstract

This study aimed to determine whether published pharmacokinetic (PK) models can adequately predict the PK profile of imatinib in a new indication, such as coronavirus disease 2019 (COVID-19). Total (bound + unbound) and unbound imatinib plasma concentrations obtained from 134 patients with COVID-19 participating in the CounterCovid study and from an historical dataset of 20 patients with gastrointestinal stromal tumor (GIST) and 85 patients with chronic myeloid leukemia (CML) were compared. Total imatinib area under the concentration time curve (AUC), maximum concentration (C_{max}) and trough concentration (C_{trough}) were 2.32-fold (95% confidence interval [CI] 1.34–3.29), 2.31-fold (95% CI 1.33–3.29), and 2.32-fold (95% CI 1.11–3.53) lower, respectivelwy, for patients with CML/GIST compared with patients with COVID-19, whereas unbound concentrations were comparable among groups. Inclusion of alpha1-acid glycoprotein (AAG) concentrations measured in patients with COVID-19 into a previously published model developed to predict free imatinib concentrations in patients with GIST using total imatinib and plasma AAG concentration measurements

(AAG-PK-Model) gave an estimated mean (SD) prediction error (PE) of −20% (31%) for total and −7.0% (56%) for unbound concentrations. Further covariate modeling with this combined dataset showed that in addition to AAG; age, body-weight, albumin, CRP, and intensive care unit admission were predictive of total imatinib oral clearance. In conclusion, high total and unaltered unbound concentrations of imatinib in COVID-19 compared to CML/GIST were a result of variability in acute phase proteins. This is a textbook example of how failure to take into account differences in plasma protein binding and the unbound fraction when interpreting PK of highly protein bound drugs, such as imatinib, could lead to selection of a dose with suboptimal efficacy in patients with COVID-19.

Study Highlights

WHAT IS THE CURRENT KNOWLEDGE ON THE TOPIC?

The pharmacokinetics (PK) of imatinib are well-described. In patients with cancer, interpatient variability in drug exposure is high; with age, weight, and acute phase protein plasma levels all being reported to influence imatinib PK; and it has been proposed that individualized therapeutic drug monitoring may help to decrease the incidence of treatment failure and toxicity in these patients. In a recent study, imatinib 400 mg was shown to improve survival and reduce duration of mechanical ventilation in patients who developed severe coronavirus disease 2019 (COVID-19).

WHAT QUESTION DID THIS STUDY ADDRESS?

In the absence of existing PK-data for imatinib in patients with COVID-19, a 400 mg total daily imatinib dose was chosen based upon effective doses used in nonclinical studies and clinical experience with imatinib in patients with cancer. We sought to identify whether we could predict PK-profiles in a new disease like COVID-19 using existing clinical PK information and use COVID-19 and chronic myeloid leukemia (CML)/gastrointestinal stromal tumor (GIST) datasets to optimally describe the exposure of imatinib in these diseases.

WHAT DOES THIS STUDY ADD TO OUR KNOWLEDGE?

This is the first population PK study of imatinib in patients with COVID-19. High total concentrations of imatinib observed in patients with COVID-19 compared to CML/GIST were a result of differences in acute phase protein plasma levels between these two indications, whereas unbound concentrations were comparable among groups. After inclusion of acute phase protein-binding as a covariate, total imatinib PK in patients with COVID-19 could be predicted by PK modeling.

HOW MIGHT THIS CHANGE DRUG DISCOVERY, DEVELOPMENT AND/OR THERAPEUTICS?

To effectively predict the dose of highly protein bound drugs to administer when existing drugs are repurposed for use in a new indication, such as COVID-19, advanced model predictions of acute phase protein plasma levels and measurement of both total and unbound drug concentrations are recommended.

INTRODUCTION

Coronavirus disease 2019 (COVID-19) is caused by infection with the severe acute respiratory syndrome-coronavirus 2 (SARS-CoV-2) virus and, in severe cases, is associated with alveolar damage, endothelial injury, and accumulation of fluids in the lungs, with the potential for respiratory failure and death. Effective treatment options for critically ill patients are still limited. In response to the COVID-19 pandemic, numerous clinical trials of repurposed drugs have been conducted. Retroviral drugs (e.g., novel retrovirals, nucleoside reverse transcriptase

inhibitors, or malaria treatments) and drugs with anti-inflammatory and immune modulation properties (e.g., dexamethasone, tocilizumab, and imatinib) have been shown to be effective for some patients.[1,2]

Imatinib is currently indicated for the treatment of chronic myelogenous leukemia (CML) and gastrointestinal stromal tumor (GIST), and other hematologic and solid neoplasms. In addition, imatinib has been shown to be a critical mediator in the regulation of endothelial permeability, attenuating vascular permeability induced by several inflammatory mediators.[3,4] In a multicenter, randomized placebo-controlled study in hospitalized patients with COVID-19 receiving supplemental oxygen (CounterCOVID), patients treated with imatinib ($N = 197$) had a significantly lower mortality and shorter duration of invasive mechanical ventilation when compared with patients receiving placebo ($N = 188$).[5]

Imatinib has as an almost complete bioavailability[6] and is metabolized by CYP3A4, forming N-desmethyl imatinib, an active metabolite.[7] Imatinib in blood is highly protein bound (>95%)[7] and binds with high affinity to alpha1-acid glycoprotein (AAG).[8] Imatinib exhibits large interindividual pharmacokinetics (PK) among patients with GIST and CML.[7-10] Total imatinib clearance could partly be explained by bodyweight, age, disease diagnosis, and volume of distribution (Vd/F) by gender according to a previous PK model (demographic-PK-model).[10,11] As critically ill patients with COVID-19 are more often men, have a higher body mass index (BMI), and are typically older, this demographic-PK-model may have utility in predicting imatinib PK to support dose selection in patients with COVID-19.

However, infections, such as COVID-19 generally increase the PK variability of drugs.[12,13] Evidence suggests that in addition to direct viral damage, uncontrolled inflammation contributes to disease severity in COVID-19 and is associated with increased pro-inflammatory cytokine release.[14,15] Interleukin-6 (IL-6) plays a crucial role, upregulating acute phase proteins such as C-reactive protein (CRP) and AAG. During severe infections, such as COVID-19, CRP levels increase at least 10-fold and AAG concentrations by two-fold.[14,15] Pro-inflammatory cytokine release may also downregulate the expression of metabolizing enzymes.[16,17] Prior studies have shown that imatinib binds with high affinity to AAG and that differences in AAG levels between patients explains around half of the interpatient variability in total and unbound imatinib exposure in patients with cancer,[8,10] suggesting that levels of AAG in patients with COVID-19 may also influence imatinib PK.

The dosing for the CounterCOVID study was based on oncologic registration data, which advocated flat dosing of 400 mg once daily (o.d.).[18] To reach steady-state concentrations on day 1, a loading dose of 800 mg was administered (half-life of 18 h).[7] The choice of 400 mg o.d. was further supported by non-clinical data demonstrating that imatinib protects against endothelial barrier dysfunction,[4] at unbound plasma concentrations within the range reported clinically in patients with CML.[19] However, given differences in systemic effects between COVID-19 infection and the licensed indication, their influence on imatinib exposure could alter its therapeutic window. We hypothesized that SARS-CoV-2 infection would increase acute phase protein levels and decrease metabolizing enzyme activity, resulting in increased total imatinib exposure in this patient population when compared with patients with CML and GIST. To test this hypothesis, raw total and unbound concentration-time profiles from patients with COVID-19 were combined with the raw data of patients with CML and GIST. Two validated PK models in CML and GIST were applied to determine whether these published PK models can adequately predict the PK profile of imatinib in new indications. In addition, PK model refinement using limited sampling clinical trial data was applied to identify clinically relevant covariates that could predict imatinib exposure in these indications and describe imatinib exposure in COVID-19, CML, and GIST.

METHODS

Study population and pharmacokinetic sample collection

Patients included in the CounterCOVID study were aged greater than 18 years and hospitalized with proven SARS-CoV-2 infection and hypoxic respiratory failure.[5]

Exclusion criteria included white blood cell count less than $4*10^9$ L^{-1}, hemoglobin (Hb) <6 g dl^{-1}, thrombocytes less than $100*10^9$ L^{-1}, and active liver disease (aspartate aminotransferase [AST] and alanine aminotransferase <5* upper limit of normal [ULN], or bilirubin >1.5*ULN). Patients using strong CYP3A4 inducers, who were pregnant or breastfeeding, were recently treated for a malignancy, or had severe comorbid heart or lung disease, were excluded. This study is registered with the EU Clinical Trials Register (EudraCT 2020–001236–10).

Patients were randomized in a 1:1 ratio to treatment with oral tablets of imatinib or placebo. Patients in the imatinib group received an 800 mg loading dose on day 1, followed by 400 mg o.d. for 9 days. Patients in the placebo group received inactive tablets. Blood samples were collected at ~ 4 and 8 h after the first dose and prior to the imatinib or placebo dose on days 1, 2, 3, 5, 7, and 9 (or until discharge). Plasma was isolated by centrifugation and stored at −80°C until analysis.

Total and unbound sample analysis

Plasma concentrations of imatinib were determined in batches using two validated liquid chromatography–tandem mass spectrometry (LC-MS/MS) methods.[20,21] The methods were cross validated at Amsterdam University Medical Centre (Amsterdam, The Netherlands) and Lausanne University Hospital (Switzerland), as part of the Pharmacological Monitoring in EUTOS for CML.[21] Plasma AAG concentrations were determined using enzyme-linked immunosorbent assay (ELISA) methodology.[22] Unbound concentrations were determined from fresh frozen samples using a validated method.[8] The validated lower limit of quantification (LLOQ) in the prior CML/GIST data was 1 μg/L[8] and in COVID-19 (in Amsterdam UMC) was 50 μg/L, with a lower limit of detection (LLOD) of 2.5 μg/L (further validation is ongoing). Samples below the LLOQ and above LLOD were included in the analyses.[23]

A representative subset of 275 plasma total concentrations from 74 patients treated with imatinib from the CounterCOVID study was used for model building (57 men/17 women). Unbound concentrations were measured in balanced subset (balanced for the time after dosing and in patients who used at least 3 doses of imatinib) of 48 samples from 38 patients. These total and unbound samples were used to validate the application of PK models developed from data obtained from patients with CML/GIST to patients with COVID-19. Another subset of 205 total plasma concentrations from 60 CounterCOVID patients was used for validation of the final PK model.

Historical datasets from CML and GIST and corresponding population PK models

We used total imatinib concentration-time profiles from rich sampled data and the corresponding population PK-models from two previously published studies[8,10] in 20 patients with CML and 85 patients with GIST (53 men/45 women). Plasma samples were collected at steady-state at varying times after dosing. Total and unbound imatinib concentrations were determined for 475 and 150 samples, respectively, with a median of four (1–10) plasma samples per patient collected over one or multiple dosing intervals. The dose at steady-state ranged between 100 and 800 mg in CML/GIST. Missing data (e.g., missing individual albumin values or bodyweights) were extracted from the original patient case report forms.

Of the two previously published models based upon these two datasets, the demographic-PK-model was built based on total concentrations in 49 patients with CML/GIST and was externally validated.[24-26] This model is a first order absorption, one-compartment model with demographic covariables bodyweight, age, disease on total apparent clearance (CL/F) and gender on Vd/F.[10] The second PK model[8,10] was based on total and unbound imatinib concentrations and AAG levels from 49 patients with GIST. This AAG-PK-model is a first order absorption, one-compartment model in which imatinib binds nonlinearly to AAG and forms a complex, with an in vitro/in vivo estimated dissociation constant K_D and linear elimination of the unbound fraction only.

Software

Castor EDC https://data.castoredc.com was used for study data management. R software (version 4.0.3; R Foundation for Statistical Computing, Vienna, Austria) was used for data-analysis, formatting, and graphical visualization. PK and covariate modeling were performed using the nonlinear mixed-effects modeling software (NONMEM version 7.3; Globomaxx LLC, Hanover, MD, USA) with Piraña Software (version 3.0; Certara) and Perl-speaks-NONMEM (PsN). The VPC package (version 1.0.1; R) was used for visual diagnostics.

Pharmacokinetic analysis

Using the demographic-PK-model in patienst with cancer (CML/GIST; Table S2),[24-26] we first evaluated whether this previously published PK-model in patients with CML/GIST could predict the observed concentrations and variability in CL/F and oral Vd/F of imatinib in patients with COVID-19. We applied the dosage and the demographic variables, as presented in Table 1, to the original PK parameters from the original models and performed 1000 simulations of the dosing regimens of the patients to predict the concentration time profiles of the full dataset (AAG-PK-model in Supplement 2). Differences in imatinib PK profiles between patients with COVID-19 and patients with CML/GIST were studied using prediction corrected visual predictive checks (VPCs). Here, we compared the observations and simulated predictions to assess the ability of the validated PK-model in CML/GIST to reproduce the central tendency and the variability in both the observed cancer and COVID-19 data.[8,10] Furthermore, we assessed the overall performance of these two models to predict concentrations among patients with cancer and patients with COVID-19 using the prediction error (PE; Equation 1).

$$PE_i = \frac{C_{pred}i - C_{obs}i}{C_{obs}i} \times 100\%$$ (1)

TABLE 1 Baseline demographics and clinical characteristics of the study groups

| | Model building set | | Validation set | Comparison cancer/ COVID-19 |
| | CML (n = 20)/GIST (n = 85) | COVID-19 patients (n = 74) | COVID-19 (n = 60) | |
	Median (IQR)	Median (IQR)	Median (IQR)	p value
Age (years)	59 (48–68)	65 (58–72)	64 (55–72)	0.0060
Male (N; %)	56 (53.3)	57 (77)	47 (78.3)	0.0019
Bodyweight (kg)	71 (61–81)	82 (77–94)	85 (76–100)	<0.0001
Height (cm)	170 (164–175)	173.5 (168–182)	175 (170–180)	0.0024
BMI (kg/m^2)	24.5 (21.9–27.4)	26.7 (24.7–29.6)	27.3 (25.2–31)	<0.0001
Smoke (no, yes, former) (N; %)		46, 2, 24 (64, 2.8, 33)	38, 2, 20 (63, 3.3, 33)	
ICU admission (N; %)	0 (0)	14 (18.9)	15 (25)	<0.0001
Administered dose at Css (mg)	400 (100–800)	400 (-)	400 (-)	
eGFR (ml/min/1.73 m^2)		87.5 (75–90)	87 (71–90)	
Albumin (g/L)	36.1 (33.1–40.0)	32.0 (28–36)	36 (33–39)	0.0008
AAG (g/L)	0.80 (0.63–1.0)	1.96 (1.6–2.3)	1.9 (1.7–2.1)	<0.0001
CRP (g/L)		0.110 (0.063–0.171)	0.109 (0.049–0.156)	
ALAT (U/L)		39.00 (26–59)	35.5 (27–45)	
ASAT (U/L)		47.00 (35–56)	45 (35–65)	
Bilirubin (mg/dl)		8.00 (6.00–10.00)	9 (7–11)	
GGT (U/L)		69.50 (39.3–107.3)	56 (36–100.5)	
Hb (mmol/L)		8.25 (7.80–8.80)	8.6 (8–9.1)	
Leukocyte (*10^{-9}/L)		6.95 (5.23–9.40)	7.4 (5.775–10.975)	
Chloroquine (N; %)	0 (0)	13 (17.6)	1 (1.67)	<0.0001
Remdesivir (N; %)	0 (0)	21 (28.4)	9 (15)	<0.0001
Dexamethasone (N; %)	0 (0)	38 (51.4)	50 (83.3)	<0.0001
ABCB1 inhibitors (N; %)	23 (21.9)	63 (85.1)	42 (70)	<0.0001
ABCG2 inhibitors (N; %)	5 (4.8)	29 (39.2)	16 (26.7)	<0.0001
OATP1A2 inhibitors (N; %)	2 (1.9)	14 (18.9)	0 (0)	<0.0001
OCT1 inhibitor (N; %)	5 (4.8)	29 (39.2)	14 (23.3)	0.0002
CYP3A4 inhibitors (N; %)	11 (10.5)	35 (47.3)	28 (46.7)	<0.0001
CYP3A4 inducers (N; %)	3 (2.9)	39 (52.7)	50 (83.3)	<0.0001
PPI (N; %)	8 (7.6)	24 (32.4)	25 (41.7)	0.0004

Note: All data are presented as median and IQR: 0.25–0.75, unless stated otherwise (N/%). Chi-square tests are used for all categorical data. Mann-Whitney U test are used for numerical data.

Abbreviations: AAG, alpha-1-acid glycoprotein; ALAT, alanine amino transaminase; ASAT, aspartate aminotransferase eGFR was calculated using Chronic Kidney Disease Epidemiology Collaboration equation (CKD-EPI); BMI, body mass index; CML, chronic myeloid leukemia; COVID-19, coronavirus disease 2019; CRP, C-reactive protein; Css, steady-state maximum concentrations; GGT, gamma glutamyl transferase; GIST, gastrointestinal stromal tumor; Hb, hemoglobin; HB, hemoglobin; ICU, intensive care unit; IQR, interquartile range; PPI, proton pump inhibitor.

Here, PE$_i$ is the individual prediction error, C_{predi} is the individual predicted concentration, and C_{obsi} is the individual observed concentration.

If the model validation suggested that the PK between CML/GIST and COVID-19 was different, further analyses were planned to identify covariates that may explain these differences. The most predictive literature-based PK model was optimized based on the CML/GIST datasets and then refitted to the total concentration-time

profiles of the joint datasets. Subsequently all parameters were re-estimated for both the patients with cancer and the patients with COVID. To optimally explore covariates reflective of total imatinib exposure, the AAG binding equation[8,10] was replaced by an alternative parametrization for the PK parameters, as described in detail in Supplement 1. After data-exploration, all continuous covariates, including AAG, were normalized to the population median values and were included after

natural log-transformation (Equation 2). In addition, for the most important covariates, linear and exponential models were tested. All population parameters were modeled on an exponential scale (i.e., estimate exp(θ), instead of θ, (Equation 2)).

$$P_i = \exp\left(\theta_P + \theta_{cov} \times \log\left(\frac{\text{covariate}_i}{\text{covariate}_{\text{median}}}\right) + \eta_{P,i}\right) (2)$$

Here, Pi is the individual parameter for subject i with covariate i. θ_P is the typical value of the population pharmacokinetic parameter. Covariate$_i$ represents the covariate, such as AAG, for subject i, and covariate$_{\text{median}}$ represents the median value of the covariate, $\eta_{P,i}$ describes the random interindividual variability. The relationship between individual empirical Bayes estimates and additional covariables of interest was examined in correlation plots using R. Body size, drug-drug interactions (DDIs), disease (COVID/GIST/CML), protein binding (AAG, CRP, and albumin), intensive care unit (ICU) admission in the 28-day study period or liver/renal failure (in all patients) were investigated to further explain the variability in K_A, CL/F, and Vd/F among patients with CML/GIST and patients with COVID-19. To assess the effect of body size on PK, BMI, adjusted bodyweight, and lean body weight (LBW) was calculated. DDIs were clustered and are displayed in Table S1. Apart from these DDIs, drugs specifically used in COVID-19 were assessed independently by hydroxychloroquine/remdesivir/dexamethasone. All relevant covariates were included using a full covariate model, followed by a backward elimination procedure.[24-26] Here, a *p* value < 0.01, corresponding to an objective function value (OFV) increase of at least 6.6 units was applied.

Model evaluation and validation

Goodness-of-fit plots and Bland Altman plots were used for diagnostic purposes. Furthermore, the PE, confidence interval of the parameter estimates, the correlation matrix, and visual inspection of the distribution of the model parameters were used to evaluate the models. Forest plots were used to define clinically significant covariates on total imatinib exposure in the combined dataset final model. Validation of the predictive value in COVID-19 of the combined dataset final model was performed by applying the model to a second CounterCOVID dataset. VPCs and mean PE, stratified for the clinically significant variables, were used to demonstrate the goodness of fit. Bias and prediction of the final model were assessed using the PE.

Simulations

To demonstrate the differences in PK profile between patients with cancer and patients with COVID-19, the combined dataset final model was used to perform Monte Carlo simulations for the full dataset at 400 mg o.d. dosing at steady-state. For every simulation, the derived PK parameters: total 0 to 24-h area under the concentration-time curve (AUC_{0-24h}) and trough concentration (C_{trough}), maximum concentration (C_{max}) were calculated. The mean, SD, and the mean difference in parameters between the diseases was calculated. In addition, four typical subjects with empirically chosen AAG values of 1, 1.5, 2, and 2.5 g/L were simulated to visualize the changes in PK as a result of acute infection.

RESULTS

Median age and bodyweight in the patients with COVID-19 (65 years and 81.75 kg; Table 1) were significantly higher compared to the patients with CML/GIST (60.3 years, 71.0 kg). AAG values were 2.3-fold higher in patients with COVID-19 (1.96 g/L) compared to patients with CML/GIST (0.84 g/L), but albumin levels were lower (32.0 g/L vs. 35.9 g/L) in patients with COVID-19 compared to patients with CML/GIST. The CounterCOVID model building dataset contained more concomitant use of hydroxychloroquine and remdesivir, whereas in the validation dataset most patients were treated with dexamethasone due to changes in COVID-19 treatment.

The raw observed total and unbound imatinib concentrations are presented in Table 2. Although dosing regimens were comparable, dose normalization of observed concentrations was not performed because CounterCOVID PK samples collected on day 1 after an 800 mg loading dose had not achieved steady-state (Css). Median total C_{trough} was 974 µg/L, and median unbound C_{trough} was 29 µg/L in patients with CML/GIST. Total C_{trough} was 2156 µg/L and unbound C_{trough} was 35.9 in patients with COVID-19 in the model building and total C_{trough} was 1791 µg/L in the validation set. Unbound concentrations were measured in 48 COVID-19 samples; of these, results from 12 samples were below the LLOQ (50 µg/L), but above the limit of detection and were estimated. The median total C_{max} was 2107 µg/L, in patients with CML/GIST and unbound C_{max} was 88.5 µg/L in patients with GIST. The median total C_{max} in patients with COVID-19 of the model building dataset was 7157 µg/L and unbound C_{max} was 89.2 µg/L. The total C_{max} in the validation set was 5983 µg/L.

TABLE 2 Observed values and PK model derived estimates of CL unbound from the GIST AAG-PK-Model[a] and other PK estimates from the combined dataset-final covariate model

Values	Parameters		CML/GIST	COVID-19 (subset 1; subset 2)			N
Observed	AAG	(g/L, IQR)	0.84 (0.69–1.12)	1.93 (1.64–2.28)[a]			98; 72; 60
	Observed total imatinib plasma concentrations						
	C_{max}	(μg/L, IQR)	2107 (1033–3801)	7157 (4358–11761); 5983 (2504–8346)[a]			92; 55; 46
	C_{trough}	(μg/L, IQR)	974 (376–1717)	2156 (738–4179); 1791 (928.4–3204)[a]			135; 99; 73
	Observed unbound imatinib plasma concentrations[b]						
	C_{max}	(μg/L, IQR)	88.50 (45–141)	80.70 (44.66–158.55)[a]			26; 20; 0
	C_{trough}	(μg/L, IQR)	29 (18–47)	38 (31.47–56.9)			41; 10; 0
Simulated	CL_u/F[a]	(L/h, IQR)	259 (388–581)	258 (385–578)			1000
Predicted	CL/F	(L/h, IQR)	12.95 (9.75–16.63)	5.14 (4.02–6.14)			74
	V/F	(L, IQR)	232.5 (176.5–283)	95.5 (78.3–105.5)			74
	K_A	(L/h, IQR)	0.506 (0.376–0.630)	0.663 (0.353–0.787)			74
	Final combined dataset-model predicted total imatinib plasma concentrations						
	C_{max}	(μg/L, 95% CI)	1902 (925–5566)	4389 (2093–8484)			1000
Simulated	C_{trough}	(μg/L, 95% CI)	763 (338–2479)	1768 (671–4056)			1000
	AUC	(μg*h/L, 95% CI)	306 (157.9–906.7)	709.2 (338.9–1364.3)			1000
	COVID			Low AAG	Medium AAG	High AAG	
Observed	AAG	(g/L, IQR)		<1.5	1.51–1.99	2–2.8	74
Simulated	Final combined dataset-model predicted total imatinib plasma concentrations						
	C_{max}	(μg/L, 95% CI)		2794.9 (1505.8–4908.4)	3934 (2446–6764)	5377 (3331–9251)	1000
	C_{trough}	(μg/L, 95% CI)		1054 (447.5–2276.5)	1560 (778–3142)	2227 (1230–4611)	1000
	AUC	(μg*h/L, 95% CI)		445.8 (244.0–785.3)	628.3 (416.2–1076.3)	872.9 (576.1–1500.0)	1000

Note: Observed values from samples collected between 2 and 5h postdose are presented as C_{max}, Samples collected greater than 20 h postdose are presented as C_{trough}. Observed data represent median (range, IQR): 0.25–0.75 values and simulated data are mean and 95% CI.

AUC, area under the total/unbound concentration time curve; CL, clearance; CL/F, oral clearance; CLu/F, oral unbound clearance; C_{max}, total or unbound maximum concentration; CML, chronic myeloid leukemia; C_{trough}, total or unbound trough concentration; F, apparent bioavailability; GIST, gastrointestinal stromal tumor; IQR, interquartile range; K_A, rate of absorption; PK, pharmacokinetic; V/F, volume of distribution.

[a]Dose normalization of the observed concentrations was not performed as day 1 CounterCOVID PK-samples were not at steady-state concentration. For optimal comparison of PK profiles among diseases, the visual predictive checks in Figure 1b,c and simulated PK profiles suffice.

[b]Unbound imatinib concentrations were determined for 48 samples; 12 samples with unbound concentrations below the limit of quantification (currently at 50 μg/L), but were above the lower limit of detection and were included in the analyses after careful consideration.

The demographic model[8,10] was applied to the three datasets (the original CML/GIST dataset,[10] a GIST dataset,[8] and the COVID-19 dataset). The original parameters of the demographic model are presented in Table S2. The CML/GIST demographic model adequately predicted concentrations in patients with CML and GIST, but poorly predicted concentration-time profiles in patients with COVID-19. The VPC (Figure 1a) shows a large underprediction of the concentration time profiles in patients with COVID-19, with an estimated mean PE of −68.6% (± SD 21%; Figure 2a). The Bland-Altman plot showed there was a clear trend for C_{trough} to be highly overestimated and C_{max} to be slightly underestimated.

During data inspection, eight samples were removed based on unlikely fit (predicted values deviated >4 times compared to the observed concentrations). To improve model predictions, we applied the published function and parameter estimates of the acute phase protein AAG binding model (AAG-PK-model) in patients with GIST. In the AAG-PK-model (Table S2, Supplement 2), where imatinib binds to AAG and unbound fraction is cleared, the prediction of the concentration-time profiles in COVID-19 was improved compared to the demographic-PK-model. The VPC (Figure 1c,d) of the AAG-PK-model shows the mean PE reduced from −68.6% to −20% (± SD 31%; Figure 2b, left). The VPC also shows that the model
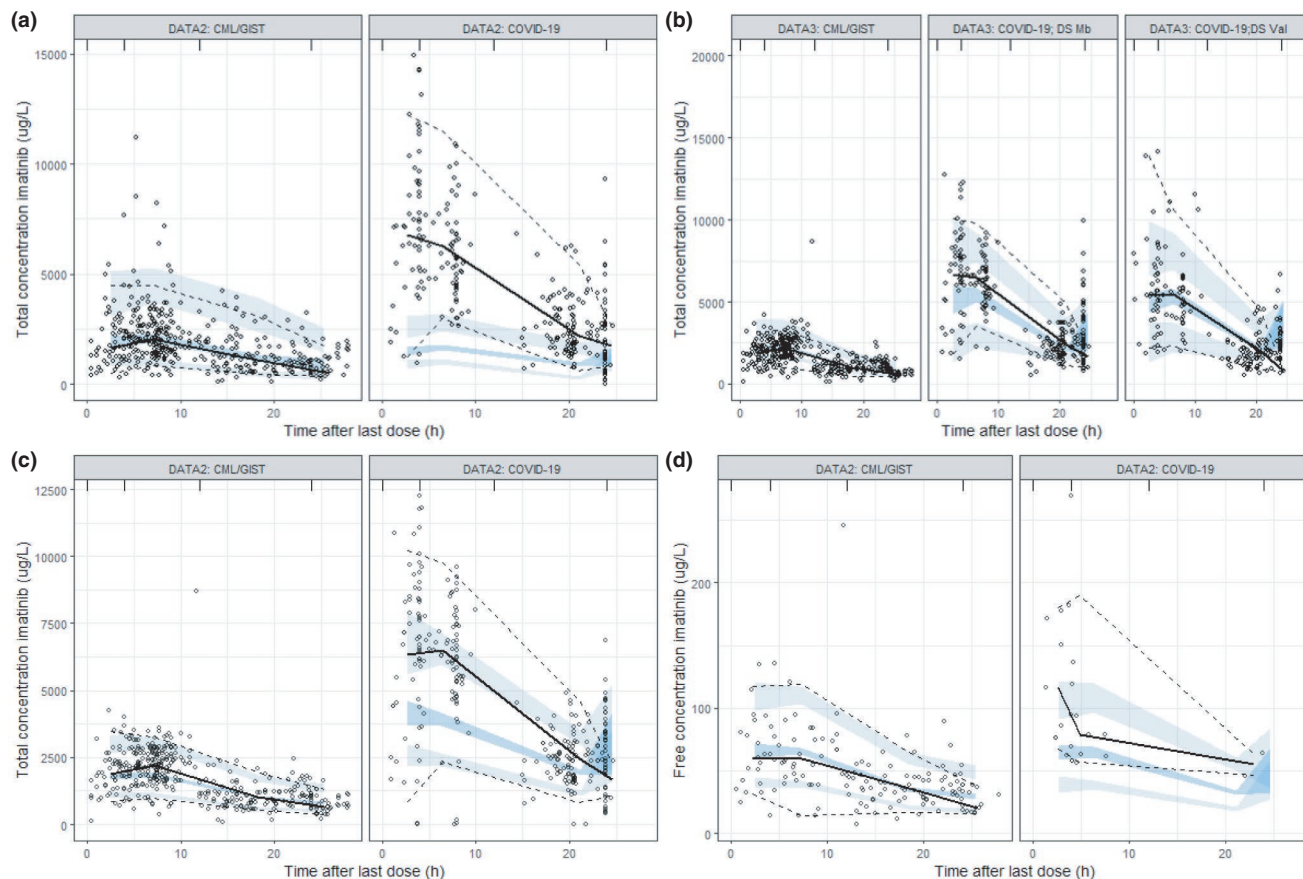
FIGURE 1 Prediction corrected, simulated imatinib concentration-time profiles in CML/GIST and COVID19 using the Demographic-PK-model (a), the model building and validation dataset using the combined dataset-final model predictions (b) and AAG-PK-Model (c-d). *1000 Simulations were performed. A VPC compares the observations and simulated predictions and can be used to assess the ability of the validated PK-models to reproduce the central tendency and the variability in the observed COVID-19 PK-data. The dots represent the observed data. The black lines represent the fifth percentile, median (solid) and 95th percentile (dashed) of observed plasma concentrations. The semitransparent dark blue field represents a simulation-based 95% confidence interval. DS-Mb: dataset used in model-building; DS-Val: dataset used in model validation. The straight grey line in plot D represents the current limit of quantification for the unbound concentration in Amsterdam UMC. CML, chronic myeloid leukemia; COVID-19, coronavirus disease 2019; GIST, gastrointestinal stromal tumor; PK, pharmacokinetic; VPC, visual predictive check

adequately predicted total C_{trough}, but underestimated total C_{max} in patients with COVID-19. In addition, the model allowed evaluation of unbound imatinib concentrations in patients with COVID-19 with a mean PE of −7% (± SD 56%) in patients with COVID-19 (Figure 2b right). The derived mean predicted clearance of unbound imatinib in CML/GIST and COVID-19 are presented in Table 2.

To further evaluate covariates predicting total imatinib exposure, K_A, CL/F, and Vd/F were estimated for patients with COVID-19 and patients with cancer (Table S2; combined dataset-base model) from the published AAG-PK-model, after model-optimization by using log-scaling as explained in Supplement 1. Covariate correlations and clinical relevance were explored in the full dataset (Figure S1). AAG, hemoglobin, bodyweight, ALAT, CRP, eGFR, albumin, smoking, ICU admission and DDIs on CL/F;

AAG, low bodyweight (LBW), gender, and albumin on Vd/F; and DDIs, AAG, albumin, and BMI on K_A were included in the combined dataset-final model. In the full-covariate analyses, imatinib concentrations decreased slightly with co-administration of CYP3A4 inducers, such as dexamethasone, whereas the ABCB1 drug transporter remdesivir had an opposing effect, increasing imatinib concentrations. However, their individual effect could not fully be differentiated, as these drugs were often co-administered (Table 1).

In the combined dataset-final model, none of the DDI covariate effects on CL/F and K_A were retained (all ΔOFV <6.6 upon backward elimination). Gender, eGFR, CRP, hemoglobin, and smoking did not influence PK (Figure S2, Table S2). The backward deletion identified ICU admission, CRP, AAG, age, bodyweight, and albumin as significant covariates for imatinib disposition in patients
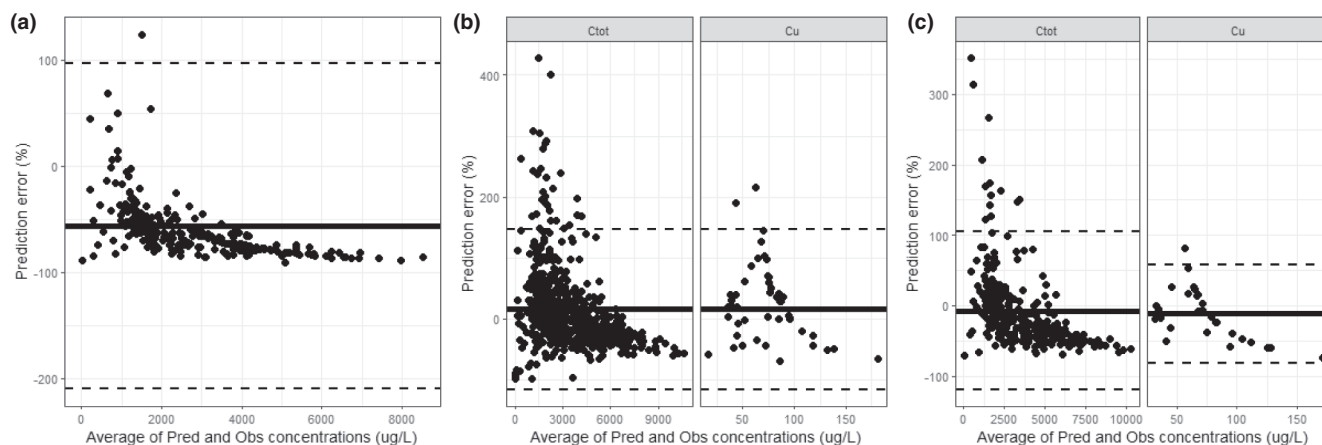
FIGURE 2 Bland-Altman plot of model predicted and observed imatinib concentrations versus the mean of predicted (Pred) and observed (Obs) concentrations in patients with COVID-19 using the CML/GIST-derived Demographic-PK-Model (a), the GIST patient-derived AAG-PK-Model, using total and unbound concentrations (b), and the model building (left) and validation dataset (right) of the combined dataset-final model (c). The lines show the mean and mean +1.96 SD of the prediction error. When not specified, total concentrations are shown. Cu = unbound concentration; Ctot = total concentration. CML, chronic myeloid leukemia; COVID-19, coronavirus disease 2019; GIST, gastrointestinal stromal tumor

with CML/GIST and patients with COVID-19. AAG explained an absolute 34% and 60% of interindividual variability (IIV) in CL/F and Vd/F, respectively, ($p < 0.0001$, ΔOFV-278; Figure 3). The forest plot of covariate effects (Figure 4) illustrates that AAG is the most clinically important variable determining imatinib exposure, as the 95% confidence interval (CI) of this covariate effect at the first and ninth quantile of the full dataset falls outside the interval of 80 to 120%. Age ($p < 0.0001$, ΔOFV = −18.6), whereas bodyweight ($p < 0.0001$, ΔOFV = −23) explained another 4.1% IIV on CL/F in the full population. Low albumin levels ($p = 0.0009$, ΔOFV-11.2), and high CRP (in patients with COVID-19 only; $p = 0.009$, ΔOFV = −6.8) predicted low CL/F. Fourteen patients were admitted to the ICU within the 28 days after treatment onset. These patients had a significantly higher CL/F (12.7 vs. 11.7 L/h) compared with patients not admitted to the ICU ($p < 0.0001$, ΔOFV = −34.7), after accounting for the effect of high AAG and low albumin values.

The forest plot suggests that albumin, ICU admission, CRP, age, and bodyweight on PK did not result in clinically significant variability in PK (Figure 4). The derived mean predicted Vd/F, CL/F, and K_A in CML/GIST and COVID-19 are presented in Table 2.

The prediction-corrected VPC plot of the combined dataset final model shows a consistent distribution of observed and predicted total imatinib concentrations between patients with cancer and patients with COVID-19 (Figure 1b). The mean PE reduced to +0.48% (± SD 45%) in the model building and +15.2% (± SD 64%) in the validation set (Figure 2c right).

The prediction corrected VPC of the combined dataset final model shows that high total imatinib exposures in

patients with COVID-19 are associated with higher concentrations of acute phase proteins (Figure 1b, Figure S3). An overview of the model and all parameter estimates in the combined dataset final model is provided in Table S2 and Supplement 3.

Simulations using the initial GIST based AAG-PK-model and the final model demonstrate the significance of inflammatory parameters on total and unbound imatinib PK. Simulations using the AAG-PK-model *s*hows that unbound concentrations remain constant, but total concentrations increase in patients with higher AAG levels (Figure 5a). Simulations of total concentrations using the combined dataset final model show that for a 400 mg dose the total AUC was 2.32-fold (95% CI 1.34–3.29) lower in patients with CML/GIST compared to patients with COVID-19: 306 µg*h/L versus 709.2 µg*h/L. Total C_{max} was 2.31-fold (95% CI 1.33–3.29) and total C_{trough} was 2.32-fold (95% CI 1.11–3.53) lower in patients with CML/GIST compared to patients with COVID-19: total C_{max} 1902 µg/L versus 4389 µg/L and total C_{trough} 763 µg/L versus 1768 µg/L, respectively (Figure 5b, Table 2). Median total C_{trough} estimates at steady-state were 1054 µg/L in patients with COVID-19 with AAG levels less than 1.5 mg/L, 1560 µg/L in patients with AAG levels 1.51–1.99 mg/L and 2227 µg/L in patients with AAG levels greater than 2 mg/L (Figure 5c, Table 2).

DISCUSSION

Median total area under the total concentration time curve (AUC), total C_{max} and total C_{trough} were 2.32-fold (95% CI 1.34–3.29), 2.31-fold (95% CI 1.33–3.29), and
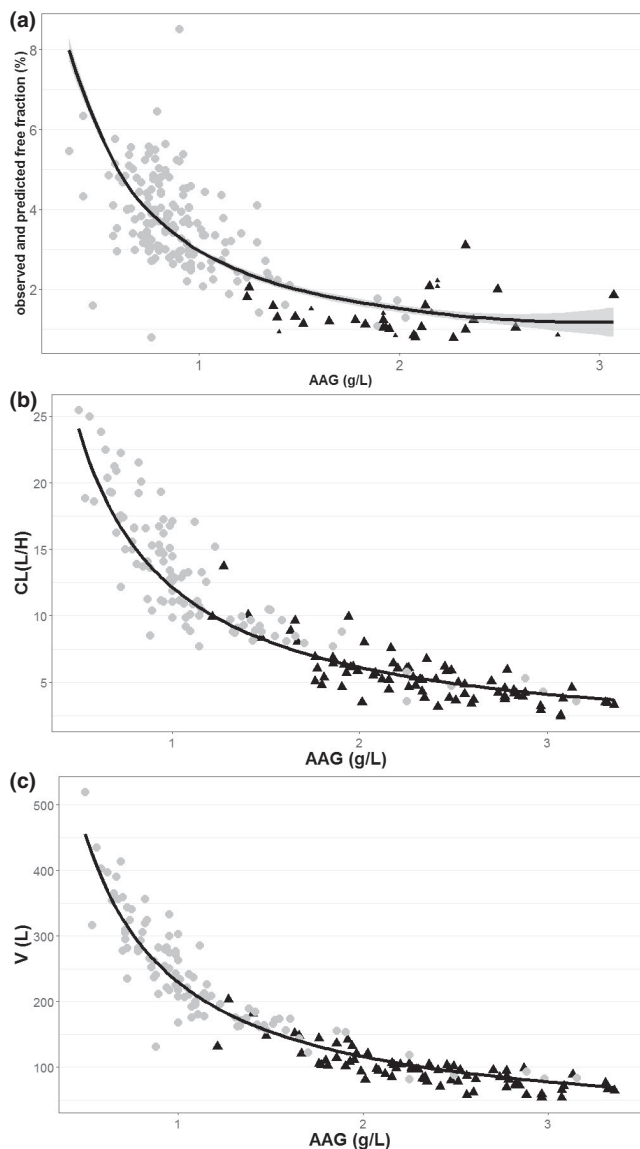
FIGURE 3 Covariate–PK relationships in GIST AAG-PK-Model and the combined dataset-final model: AAG – free fraction (a) AAG – oral clearance (b), AAG – volume of distribution (c). The black lines represent the typical (mean) parameter, individual predicted values of CML/GIST (grey dots) and COVID-19 (black triangles). In figure A the 12 small triangles are derived from the BLOQ unbound concentrations. BLOQ, below the limit of quantification; CL, clearance; CML, chronic myeloid leukemia; COVID-19, coronavirus disease 2019; GIST, gastrointestinal stromal tumor; L/H, low/high; PK, pharmcokinetic; V, volume

2.32-fold (95% CI 1.11–3.53) lower, respectively, for patients with CML/GIST compared with patients with COVID-19, whereas unbound concentrations were comparable among groups. Pooling of previously published PK models of imatinib and data obtained after PK sampling in three studies predicted variability in imatinib PK among diseases and were able to quantify the difference in exposure between patients with COVID-19 and patients with CML/GIST. The final PK-model showed that

the higher total imatinib exposure observed in patients with COVID-19 compared with patients with CML/GIST is the result of differences in acute phase protein concentrations: higher AAG and, to a minor extent, higher CRP and lower albumin levels.

Simulations using the AAG-PK-model,[8] demonstrated that unbound imatinib determined the rate of elimination of imatinib in patients with cancer and patients with COVID-19. However, the underprediction of total C_{max} by the mechanistic AAG-PK-model suggests that increased protein binding is not the only factor influencing PK of imatinib in COVID-19. High plasma levels of acute phase proteins may also indirectly affect metabolism of imatinib. Imatinib is primarily metabolized by CYP3A4, forming an equally active metabolite: N-demethylated piperazine derivative (~ 10% of the parent AUC).[7] Only 68% of the drug is excreted via the feces and only 13% by renal excretion, of which 25% is unchanged. High acute phase proteins may downregulate cytochrome P450 enzymes (CYPs) in the gut and liver by transcriptional suppression of CYP mRNA, triggering a decrease in enzyme synthesis.[16,17] Prior studies have hypothesized that CYP inhibition may occur during SARS-CoV-2 infection, potentially as a direct effect of immune modulation on the formation of metabolizing enzymes in systemic hyperinflammation associated with severe disease states.[27] Low albumin may reflect disease severity. The observed effect of albumin on imatinib clearance suggests that hepatic metabolism and/or enterohepatic circulation may be decreased and fecal excretion reduced in severely diseased patients due to inhibition of liver- and gut-enzymes. Future research should explore whether immune activation results in an increase in plasma protein concentrations and CYP3A4 inhibition, and how both affect imatinib PK. These studies should include measurement of imatinib metabolites and endogenous CYP3A4/5 activity biomarkers such as 4β-hydroxycholesterol.[28]

The observed positive correlation between the selected covariates and imatinib exposure are in line with previously published data.[8,10] Imatinib is highly protein bound (>95%[7]) with high affinity for AAG (KD of 327.0 ± SD 7.9 μg/L[8]) and with an affinity for albumin (KD 4580 ± SD 144 μg/L) and CRP[8] ~ 50–60 times lower. Previously, in patients with moderate to severe renal failure, high total imatinib concentrations and increased AAG values were observed.[29] Although the increase in imatinib clearance with bodyweight in this study could be explained by increased cardiac output, renal or liver blood flow, and liver size relative to weight; age and bodyweight do not appear to appreciably impact imatinib PK. In patients with COVID-19 with higher BMI or older age than included in this study (BMI ≤40 mg/m² and median age 65 years), effects of bodyweight and age on clearance may be different. Patients with COVID-19 with BMI above 35 kg/m² or
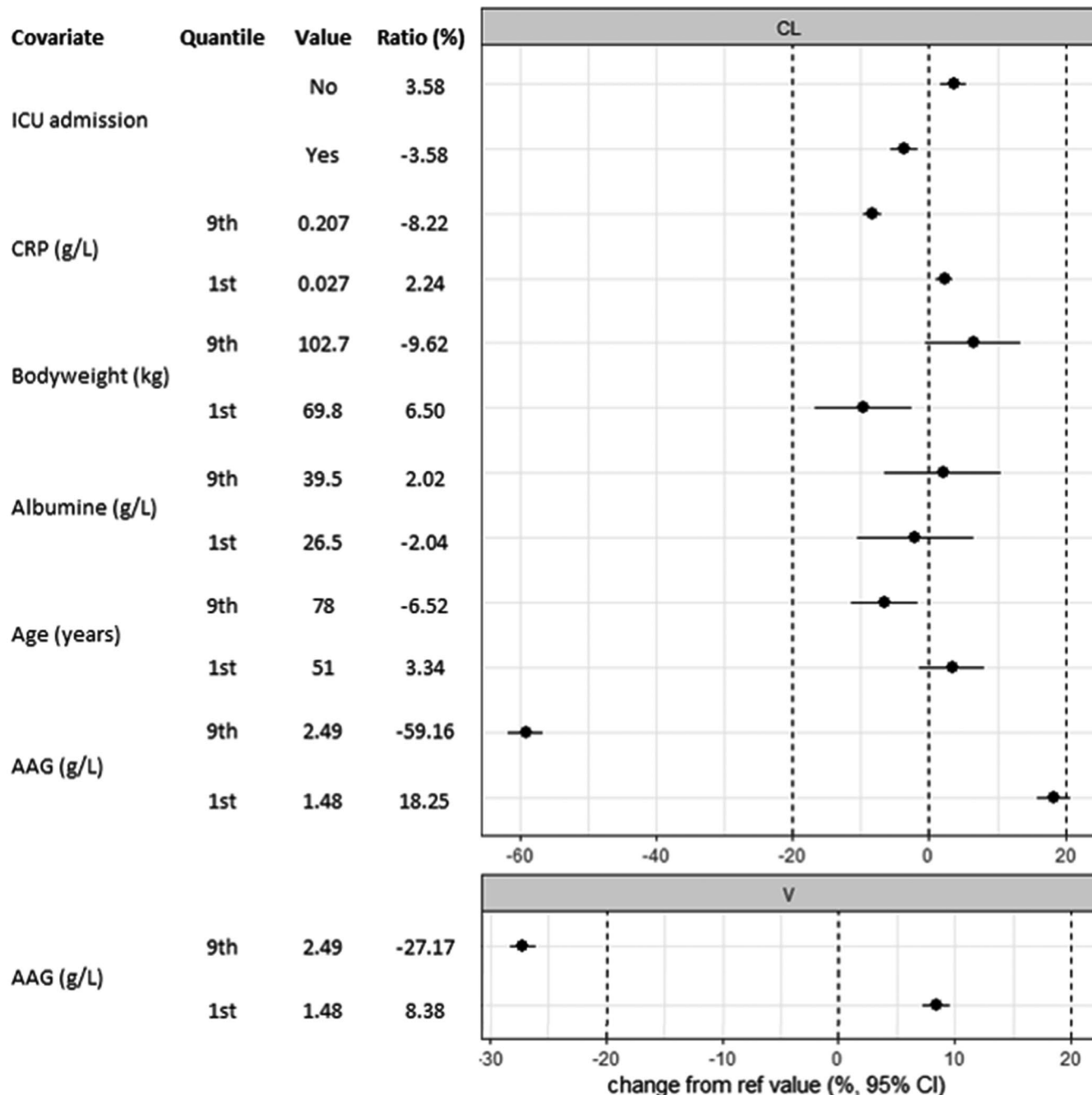
FIGURE 4 Forest plot for covariates on total imatinib exposure in the combined dataset-final model. Figure shows the mean and 95% CIs of clearance (CL) and volume (V), relative to the reference values for these PK parameters obtained using fixed-effects models. The 80–120% lines are shown to demonstrate clinical relevance. Q1/Q9 are the first and nineth quantiles of the deviations from the median value observed in the COVID-19 dataset. CI, confidence interval; COVID-19, coronavirus disease 2019; ICU, intensive care unit; PK, pharmacokinetic

older than 75 years treated with imatinib should be closely monitored and dose reduction should be considered in the presence of treatment-limiting side effects. Clinically relevant interactions between imatinib and concomitant medications specifically used to treat COVID-19 were ruled out as causes for high total imatinib exposure. No interaction with CYP3A4 or drug transporters were observed, similar to prior imatinib PK studies.[7-10,30] However, strong inducers were prohibited in the trial. Drugs in were often combined (e.g., remdesivir [ABCB1/ABCG2 inhibitor] with dexamethasone [CYP3A4 inducer]) in these patients and the COVID-19 treatment plan evolved over time, limiting the individual DDI assessment. Although some concomitant medications changed, no differences in concentration time profiles between the CounterCOVID model building and validation dataset was observed.
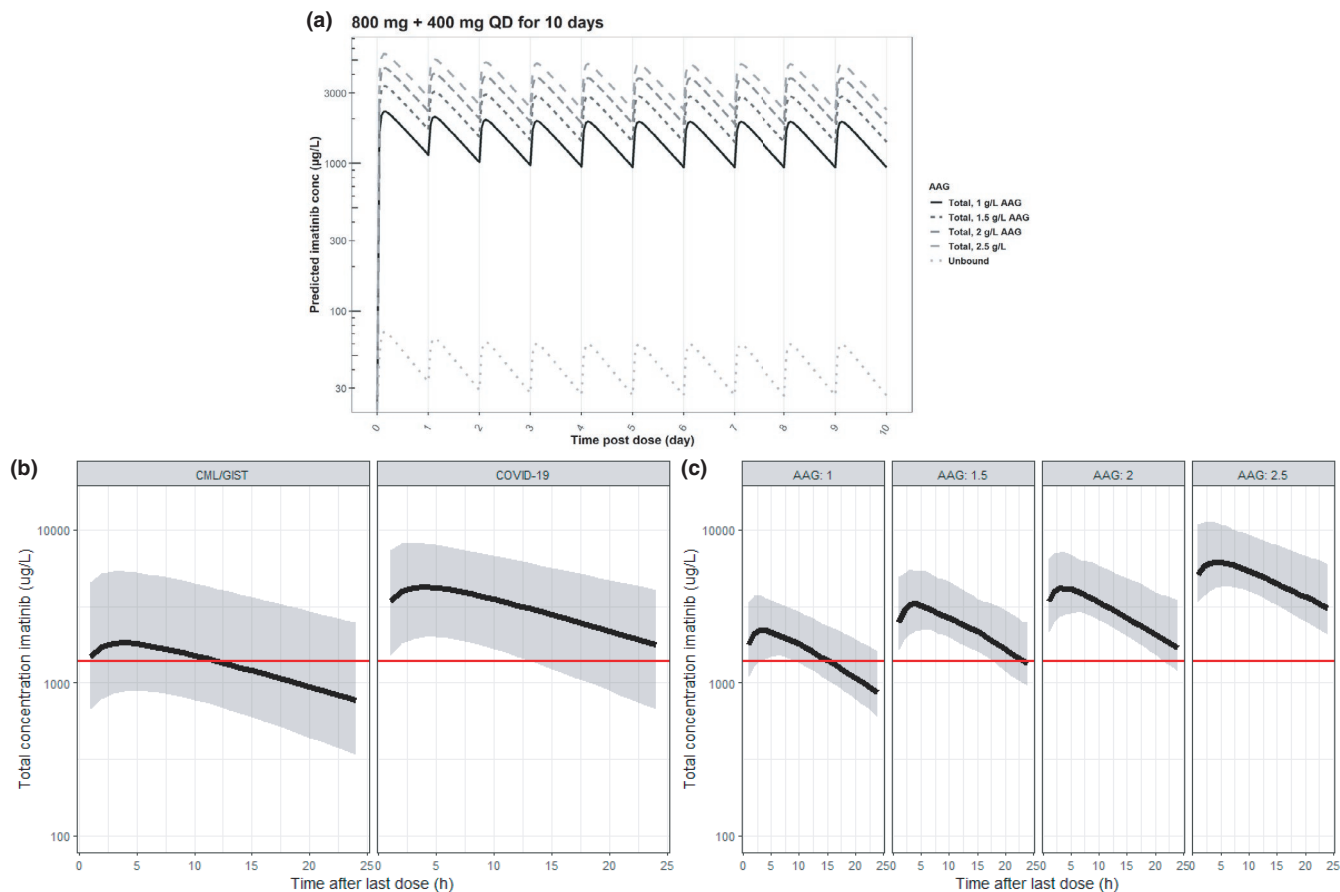
FIGURE 5 Simulation of the total and unbound concentration-time profiles in a typical cancer or COVID-19 patient with varying AAG levels using historic AAG-PK-Model (a); in patients with COVID-19 compared with patients with CML and GIST at 400 mg daily dosing at steady-state using the combined dataset-final model (b); in patients with COVID-19 with varying AAG levels using the combined dataset-final model within (c). IQR = interquartile range: 0.25–0.75. The black lines and semitransparent dark grey fields represent the median and 95th percentile of the simulated data. The red line references the in vitro observed minimal effective concentration that protects the endothelial barrier (1400 µg/L total and 60 µg/L unbound concentration).[4] CML, chronic myeloid leukemia; COVID-19, coronavirus disease 2019; GIST, gastrointestinal stromal tumor

To our knowledge, this is the first study demonstrating high and highly variable AAG-levels in combination with high total concentrations of imatinib in patients with COVID-19. Infection with SARS-CoV-2 releases inflammatory cytokines, such as IL-6 and activates intracellular signaling cascades, potentially leading to increased IL-6 production and subsequent increase in acute phase proteins such as CRP and AAG.[31] Correlations between elevated IL-6 and increases in exposure to the antiviral drugs darunavir and lopinavir have been reported in patients with COVID-19.[31,32] In these studies, lopinavir/ritonavir and darunavir total exposure increased 2–5-fold in patients with COVID-19 compared with non-COVID-19 patients[31,32]; whereas, similar to our observations with imatinib; unbound concentrations remained unaltered compared to patients with HIV.[33] HIV protease inhibitors are similar to imatinib, in that they are predominantly bound to AAG.[34] Levels of the acute phase protein CRP correlated with total plasma levels of lopinavir/

ritonavir in patients with COVID-19.[32] In infectious diseases beyond COVID-19, similar associations have been reported for multiple drugs with high protein binding (>90%), where there is relatively high AAG and lower albumin binding[13] (e.g., antipsychotics, midazolam, and voriconazole).[35-37] A clozapine study also suggest that free drug fractions may be lower in patients with high AAG levels.[38] Interestingly, in the 14 CounterCOVID patients who were admitted to the ICU during the study, total imatinib clearance was higher and total imatinib exposure lower than in patients who stayed on the ward - after accounting for the effect of acute phase proteins on total PK. This finding needs further exploration, but could suggest that patients with low exposure had a higher AAG, higher inflammatory cytokine activity, and consequently greater endothelial permeability, leading to the development of more critical disease and ICU admission. However, other biomarkers potentially predictive of disease progression: low albumin levels and high CRP predicted low CL/F and

high exposure.[39] Therefore, future PK/pharmacodynamic (PD) studies of imatinib should assess the correlation with disease severity.

For drugs with a narrow therapeutic window, such as imatinib, high PK-variability may have serious implications on clinical outcomes. Multiple studies have shown correlations between imatinib exposure and efficacy in patients with cancer,[40-47] with only 50% of patients after standard 400 mg daily dosing reaching a total C_{trough} above the 1000 µg/L target total concentration required for efficacy.[40] Median total imatinib exposures (total C_{trough}, AUC, and C_{max}) were 2.3-fold higher in patients infected with SARS-CoV-2 than those reported historically in patients with CML/GIST. The higher total imatinib exposure in patients with COVID-19 in the CounterCOVID study was not associated with increases in the incidence or severity of side effects reported in cancer studies[40-47] and no new adverse events were identified, despite a report of a correlation between unbound imatinib exposure and toxicity in patients with CML/GIST.[48] Imatinib is proposed to exert its biological effect in COVID-19 by binding to the cytosolic tyrosine-protein kinase ABL2, to attenuate vascular permeability and its efficacy is dependent upon the unbound drug concentration at the site of action, as only unbound drug is able to distribute from the systemic circulation across membranes to tissues. Unbound concentrations of imatinib were similar to those reported in patients with CML/GIST.

Given the similarities in unbound imatinib concentrations and binding affinities for its different intracellular targets in CML/GIST and COVID-19 (ABL1 and ABL2, respectively), imatinib doses used in the treatment of CML/GIST would be expected to be efficaceous in the treatment of COVID-19, despite the higher total imatinib concentrations observed in COVID-19. Higher doses may improve efficacy but may increase the risk toxicity. Unbound concentrations in patients with COVID-19 reach the *in vitro* determined unbound half-maximal inhibitory concentration (IC_{50}) of ~ 50 ug/L (total 1900 ug/L; and estimated 3.2% unbound fraction) for endothelial barrier protection,[4,49] 2 h after a loading dose of 800 mg. 400 mg–800 mg q.d. dosing maintains this concentration near the IC_{50} 2 h after a loading dose of 800 mg, 400 mg–800 mg q.d. dosing maintain this concentration near the IC_{50}. Higher doses (800 to 1000 mg) are applied in germatofibrosarcoma protuberans, GIST with KIT exon-9 mutations and some patients with glioblastoma multiforme.[50] However, dose/concentration-toxicity studies suggest that doses above 600 mg and high unbound concentrations may increase toxicity.[10,48] In CounterCOVID, more imatinib treated patients stopped treatment prematurely during to gastrointestinal (GI) toxicity.[5] For this reason, we consider 800 mg loading and 400 mg q.d. the optimal dose, with higher doses based on therapeutic drug monitoring

(TDM) of the unbound concentration to be considered in case of severely diseased patients with COVID-19.

Continued exploration of imatinib PK is of significant interest for the treatment of COVID-19. Patients in the CounterCOVID study treated with imatinib ($N = 197$) had a significantly lower mortality and shorter duration of invasive mechanical ventilation when compared with patients receiving placebo ($N = 188$).[5] Following these results, four new multicenter trials with imatinib are currently recruiting; p.o. imatinib in Solidarity by the World Health Organization (WHO) and the REMAP-CAP study[51]; and i.v. imatinib in the INVENT-COVID and IMPRESS studies.[52]

The main limitations of this study are the small number of free fraction determinations (22 patients with values above the current quantification limit) and relatively few PK-samples and AAG-measurements beyond day 5. AAG and imatinib concentrations may change over the treatment period. Imatinib may decrease IL-6 and hence reduce AAG formation.[53] A prior study in patients with GIST showed total imatinib exposure reduced over time by 29.3% after 90 days of treatment[54] and reduced inflammation as a consequence of treatment efficacy and/or resolution of the effects of GIST surgery.[55] A further limitation is the applied AAG-PK-model estimates of C_u and derived C_{total}, which was reliant upon unbound K_A and unbound Vd/F. The potential for unidentified changes in unbound PK over time limit our current ability to extrapolate our findings to predict the full PK-profile in all CounterCOVID patients. Analysis of additional samples and further method validation are planned. Studies to investigate the effect of changes in plasma AAG-levels during treatment on unbound imatinib PK and the exposure-response relationship will be performed, with the objective of identifying whether a TDM strategy to optimize imatinib treatment for patients with COVID-19 would be beneficial.

In conclusion, we have demonstrated that whereas total imatinib exposure was increased in patients with COVID-19, unbound imatinib exposure was similar to that observed in patients with cancer, when repurposing existing therapies for a new indication, such as COVID-19. The potential for differences in acute phase plasma proteins and other patient characteristics, such as age, bodyweight, and disease severity should be taken into account when deciding on dose, particularly for highly protein bound drugs whose PK may be affected by the presence of inflammation. Failure to take account differences in plasma protein binding when interpreting PK of highly protein bound drugs, such as imatinib, could lead to selection of a dose with suboptimal efficacy in patients with COVID-19.

advice during preparation of this manuscript. Dr. Amina Haouala is also warmly thanked for providing the authors with the raw data of her previous work on free imatinib PK modeling. This project has received funding from the Innovative Medicines Initiative 2 Joint Undertaking under grant agreement No [101005142]. This Joint Undertaking receives support from the European Union's Horizon 2020 research.

CONFLICT OF INTEREST

S.S. is an employee of Exvastat Ltd. and has no other conflicts of interest. J.A. is an inventor on a patent (WO2012150857A1, 2011) covering protection against endothelial barrier dysfunction through inhibition of the tyrosine kinase abl-related gene (arg). J.A. has served as non-compensated scientific advisor for Exvastat Ltd. All other authors declared no competing interests for this work.

AUTHOR CONTRIBUTIONS

All authors wrote the manuscript. I.H.B., P.M.B., N.W., M.G., E.D., R.H., A.E., I.P.E.T., H.J.B., J.A., and E.L.S. designed the research. All authors performed the research. I.H.B., P.M.B., B.G., R.H., A.E., I.P.E.T., H.H., L.A.D., H.J.B., J.A., and E.L.S. analyzed the data. I.H.B., B.G., R.H., H.H., L.A.D., H.J.B., and J.A. contributed new reagents/analytical tools.

REFERENCES

1. Sharma A, Ahmad Farouk I, Lal SK. COVID-19: a review on the novel coronavirus disease evolution, Transmission, Detection, Control and Prevention. *Viruses*. 2021;13:202.
2. Salian VS, Wright JA, Vedell PT, et al. COVID-19 transmission, current treatment, and future therapeutic strategies. *Mol Pharm*. 2021;18:754–771.
3. Rizzo AN, Sammani S, Esquinca AE, et al. Imatinib attenuates inflammation and vascular leak in a clinically relevant two-hit model of acute lung injury. *Am J Physiol Lung Cell Molecul Physiol*. 2015;309:L1294-L1304.
4. Aman J, van Bezu J, Damanafshan A, et al. Effective treatment of edema and endothelial barrier dysfunction with imatinib. *Circulation*. 2012;126:2728-2738.
5. Aman J, Duijvelaar E, Botros L, et al. Imatinib in patients with severe COVID-19: a randomised, double-blind, placebo-controlled, clinical trial. *Lancet Respir Med*. 2021;9:957-968.
6. Peng B, Dutreix C, Mehring G, et al. Absolute bioavailability of imatinib (Glivec®) orally versus intravenous infusion. *J Clin Pharmacol*. 2004;44:158-162.
7. Peng B, Lloyd P, Schran H. Clinical pharmacokinetics of imatinib. *Clin Pharmacokinet*. 2005;44:879-894.
8. Haouala A, Widmer N, Guidi M, et al. Prediction of free imatinib concentrations based on total plasma concentrations in patients with gastrointestinal stromal tumours. *Br J Clin Pharmacol*. 2013;75:1007-1018.
9. van Erp NP, Gelderblom H, Karlsson MO, et al. Influence of CYP3A4 inhibition on the steady-state pharmacokinetics of imatinib. *Clin Cancer Res*. 2007;13:7394-7400.
10. Widmer N, Decosterd LA, Csajka C, et al. Population pharmacokinetics of imatinib and the role of α1-acid glycoprotein. *Br J Clin Pharmacol*. 2006;62:97-112.
11. Gotta V, Widmer N, Montemurro M, et al. Therapeutic drug monitoring of imatinib: Bayesian and alternative methods to predict trough levels. *Clin Pharmacokinet*. 2012;51:187-201.
12. Morgan E. Impact of infectious and inflammatory disease on cytochrome P450–mediated drug metabolism and pharmacokinetics. *Clin Pharmacol Ther*. 2009;85:434-438.
13. Smith SA, Waters NJ. Pharmacokinetic and pharmacodynamic considerations for drugs binding to alpha-1-acid glycoprotein. *Pharm Res*. 2019;36:30.
14. Hsiao SY, Lai Y-R, Kung C-T, et al. α-1-acid glycoprotein concentration as an outcome predictor in adult patients with sepsis. *Biomed Res Int*. 2019;2019:3174896.
15. van Beek DEC, Königs MHH, Kuijpers YAM, van der Horst ICC, Scheeren TWL. Predictive value of serum albumin levels on noradrenaline and fluid requirements in the first 24 h after admission to the Intensive Care Unit — a prospective observational study. *J Crit Care*. 2018;47:99-103.
16. Renton KW. Regulation of drug metabolism and disposition during inflammation and infection. *Expert Opin Drug Metab Toxicol*. 2005;1:629-640.
17. Dickmann LJ, Patel SK, Rock DA, Wienkers LC, Slatter JG. Effects of interleukin-6 (IL-6) and an anti-IL-6 monoclonal antibody on drug-metabolizing enzymes in human hepatocyte culture. *Drug Metab Dispos*. 2011;39:1415-1422.
18. Glivec® (imatinib) Summary of Product Characteristics - Glivec 400 mg Film Coated Tablets. https://www.glivec.com/globa lassets/site-components304/oncology/glivec/glivec-eusmpc--400mgtablets.pdf.
19. Peng B, Hayes M, Resta D, et al. Pharmacokinetics and pharmacodynamics of imatinib in a phase I trial with chronic myeloid leukemia patients. *J Clin Oncol*. 2004;22:935-942.
20. Haouala A, Zanolari B, Rochat B, et al. Therapeutic drug monitoring of the new targeted anticancer agents imatinib, nilotinib, dasatinib, sunitinib, sorafenib and lapatinib by LC tandem mass spectrometry. *J Chromatogr B Analyt Technol Biomed Life Sci*. 2009;877:1982-1996.
21. Bouchet S, Titier K, Moore N, et al. Therapeutic drug monitoring of imatinib in chronic myeloid leukemia: experience from 1216 patients at a centralized laboratory. *Fundam Clin Pharmacol*. 2013;27:690-697.
22. ALPCO Alpha 1-Acid Glycoprotein ELISA. https://www.alpco.com/store/alpha-1-acid-glycoprotein-elisa.html.
23. Keizer RJ, Jansen RS, Rosing H, et al. Incorporation of concentration data below the limit of quantification in population pharmacokinetic analyses. *Pharmacol Res Perspect*. 2015;3:e00131.
24. Lindbom L, Pihlgren P, Jonsson N. PsN-toolkit – a collection of computer intensive statistical methods for non-linear mixed effect modeling using NONMEM. *Comput Methods Programs Biomed*. 2005;79:241-257.
25. Karlsson MO, Savic RM. Diagnosing model diagnostics. *Clin Pharmacol Ther*. 2007;82:17-20.
26. Sheiner LB, Ludden TM. Population pharmacokinetics/dynamics. *Annu Rev Pharmacol Toxicol*. 1992;32:185-209.
27. El-Ghiaty MA, Shoieb SM, El-Kadi AOS. Cytochrome P450-mediated drug interactions in COVID-19 patients: current findings and possible mechanisms. *Med Hypotheses*. 2020;144:110033.

28. Gravel S, Chiasson J, Gaudette F, Turgeon J, Michaud V. Use of 4β-hydroxycholesterol plasma concentrations as an endogenous biomarker of CYP3A activity: clinical validation in individuals with type 2 diabetes. *Clin Pharmacol Ther.* 2019;106:831-840.

29. Gibbons J, Egorin MJ, Ramanathan RK, et al. Phase I and pharmacokinetic study of imatinib mesylate in patients with advanced malignancies and varying degrees of renal dysfunction: A study by the national cancer institute organ dysfunction working group. *J Clin Oncol.* 2008;26:570-576.

30. Haouala A, Widmer N, Duchosal MA, et al. Drug interactions with the tyrosine kinase inhibitors imatinib, dasatinib, and nilotinib. *Blood.* 2011;117:75-87.

31. Cojutti PG, Londero A, Della Siega P, et al. Comparative population pharmacokinetics of darunavir in SARS-CoV-2 patients vs. HIV patients: the role of interleukin-6. *Clin Pharmacokinet.* 2020;59:1251-1260.

32. Marzolini C, Stader F, Stoeckle M, et al. Effect of systemic inflammatory response to SARS-CoV-2 on lopinavir and hydroxychloroquine plasma concentrations. *Antimicrob Agents Chemother.* 2020;64:e01177-20.

33. Stanke-Labesque F, Concordet D, Djerada Z, et al. Neglecting plasma protein binding in COVID-19 patients leads to a wrong interpretation of lopinavir overexposure. *Clin Pharmacol Ther.* 2021;109:1030-1033.

34. Jones K, Hoggard PG, Khoo S, Maher B, Back DJ. Effect of α 1-acid glycoprotein on the intracellular accumulation of the HIV protease inhibitors saquinavir, ritonavir and indinavir in vitro. *Br J Clin Pharmacol.* 2001;51:99-102.

35. Hefner G, Shams MEE, Unterecker S, Falter T, Hiemke C. Inflammation and psychotropic drugs: the relationship between C-reactive protein and antipsychotic drug levels. *Psychopharmacology.* 2016;233:1695-1705.

36. Vreugdenhil B, van der Velden WJFM, Feuth T, et al. Moderate correlation between systemic IL-6 responses and CRP with trough concentrations of voriconazole. *Br J Clin Pharmacol.* 2018;84:1980-1988.

37. Kojima T, Yabe Y, Kaneko A, et al. Monitoring C-reactive protein levels to predict favourable clinical outcomes from tocilizumab treatment in patients with rheumatoid arthritis. *Mod Rheumatol.* 2013;23:977-985.

38. Man WH, Wilting I, Heerdink ER, et al. Unbound fraction of clozapine significantly decreases with elevated plasma concentrations of the inflammatory acute-phase protein alpha-1-acid glycoprotein. *Clin Pharmacokinet.* 2019;58:1069-1075.

39. Samprathi M, Jayashree M. Biomarkers in COVID-19: an up-to-date review. *Front Pediatrics.* 2020;8:607647.

40. Larson RA, Druker BJ, Guilhot F, et al. Imatinib pharmacokinetics and its correlation with response and safety in chronic-phase chronic myeloid leukemia: a subanalysis of the IRIS study. *Blood.* 2008;111:4022-4028.

41. Cortes JE, Egorin MJ, Guilhot F, Molimard M, Mahon FX. Pharmacokinetic/pharmacodynamic correlation and blood-level testing in imatinib therapy for chronic myeloid leukemia. *Leukemia.* 2009;23:1537-1544.

42. Demetri GD, Wang Y, Wehrle E, et al. Imatinib plasma levels are correlated with clinical benefit in patients with unresectable/metastatic gastrointestinal stromal tumors. *J Clin Oncol.* 2009;27:3141-3147.

43. Picard S, Titier K, Etienne G, et al. Trough imatinib plasma levels are associated with both cytogenetic and molecular responses to standard-dose imatinib in chronic myeloid leukemia. *Blood.* 2007;109:3496-3499.

44. Kantarjian HM, Cortes J, La Rosée P, Hochhaus A. Optimizing therapy for patients with chronic myelogenous leukemia in chronic phase. *Cancer.* 2010;116:1419-1430.

45. Awidi A, Ayed AO, Bsoul N, et al. Relationship of serum imatinib trough level and response in CML patients: long term follow-up. *Leuk Res.* 2010;34:1573-1575.

46. Li-Wan-Po A, Farndon P, Craddock C, Griffiths M. Integrating pharmacogenetics and therapeutic drug monitoring: optimal dosing of imatinib as a case-example. *Eur J Clin Pharmacol.* 2010;66:369-374.

47. Singh N, Kumar L, Meena R, Velpandian T. Drug monitoring of imatinib levels in patients undergoing therapy for chronic myeloid leukaemia: comparing plasma levels of responders and non-responders. *Eur J Clin Pharmacol.* 2009;65:545-549.

48. Widmer N, Decosterd LA, Leyvraz S, et al. Relationship of imatinib-free plasma levels and target genotype with efficacy and tolerability. *Br J Cancer.* 2008;98:1633-1640.

49. Okuda K, Weisberg E, Gilliland DG, Griffin JD. ARG tyrosine kinase activity is inhibited by STI571. *Blood.* 2001;97:2440-2448.

50. Reardon DA, Desjardins A, Vredenburgh JJ, et al. Safety and pharmacokinetics of dose-intensive imatinib mesylate plus temozolomide: phase 1 trial in adults with malignant glioma. *Neuro-Oncology.* 2008;10:330–340.

51. Ledford H. International COVID-19 trial to restart with focus on immune responses [published online ahead of print May 5, 2021]. *Nature.* 10.1038/d41586-021-01090-z

52. Aman J. Intravenous Imatinib in Mechanically Ventilated COVID-19 Patients - Full Text View - ClinicalTrials.gov. https://clinicaltrials.gov/ct2/show/NCT04794088.

53. Ciarcia R, Vitiello MT, Galdiero M, et al. Imatinib treatment inhibit IL-6, IL-8, NF-KB and AP-1 production and modulate intracellular calcium in CML patients. *J Cell Physiol.* 2012;227:2798-2803.

54. Eechoute K, Fransson MN, Reyners AK, et al. A long-term prospective population pharmacokinetic study on imatinib plasma concentrations in GIST patients. *Clin Cancer Res.* 2012;18:5780-5787.

55. Chatelut E, Gandia P, Gotta V, Widmer N. Long-term prospective population PK study in GIST patients - Letter. *Clin Cancer Res.* 2013;19:949.

SUPPORTING INFORMATION

Additional supporting information may be found in the online version of the article at the publisher's website.